

Optimum tilt and azimuth of fixed grid-connected photovoltaic system for peak load shaving

A multi-scale model

Bakhshi-Jafarabadi, Reza; Doh Dinga, Christian

10.1016/j.renene.2025.123714

Publication date

Document Version Final published version

Published in Renewable Energy

Citation (APA)

Bakhshi-Jafarabadi, R., & Doh Dinga, C. (2025). Optimum tilt and azimuth of fixed grid-connected photovoltaic system for peak load shaving: A multi-scale model. *Renewable Energy*, *255*, Article 123714. https://doi.org/10.1016/j.renene.2025.123714

Important note

To cite this publication, please use the final published version (if applicable). Please check the document version above.

Copyright

Other than for strictly personal use, it is not permitted to download, forward or distribute the text or part of it, without the consent of the author(s) and/or copyright holder(s), unless the work is under an open content license such as Creative Commons.

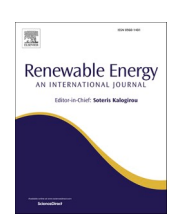
Please contact us and provide details if you believe this document breaches copyrights. We will remove access to the work immediately and investigate your claim.

ELSEVIER

Contents lists available at ScienceDirect

Renewable Energy

journal homepage: www.elsevier.com/locate/renene



Optimum tilt and azimuth of fixed grid-connected photovoltaic system for peak load shaving: a multi-scale model

Reza Bakhshi-Jafarabadi *0, Christian Doh Dinga 0

Faculty of EEMCS, Delft University of Technology, Mekelweg 4, 2628CD, Delft, the Netherlands

ARTICLE INFO

Keywords:
Azimuth
Grid-connected photovoltaic system
Optimization
Peak load shaving
Tilt

ABSTRACT

Peak load shaving is a practical alternative to over-designing the power system to meet maximum demand. In this context, grid-connected photovoltaic system (GCPVS) is an effective solution across regional and national scales. The tilt (β) and azimuth (ψ) angles of fixed-structure GCPVS are conventionally optimized to ensure maximum annual yield or minimum electricity costs. This highlights a gap that no existing study has optimized the orientation of PV modules from a peak load shaving perspective. To address this gap, for the first time, this paper proposes a multi-scale, search-based optimization methodology to determine the tilt and azimuth angles for maximizing peak load shaving. The proposed approach is applied to a 10 kW GCPVS at two commercial buildings in Delft, Netherlands, and Mashhad, Iran. The method finds $\beta = 24^{\circ}$ and $\psi = 45^{\circ}$ as an optimum solution in Delft with a heating-dominated load during cold afternoons. For Mashhad, the GCPVS shaves summer noon air conditioning-based peak load with $\beta=12^\circ$ and $\psi=-10^\circ$. The results highlight that the proposed method ensures maximum peak load shaving of the GCPVS, even with a non-optimized annual energy yield. Also, the substantial dependency of the optimal angles on the local load profile, GCPVS characteristics, and the site's solar potential is demonstrated. Although the effectiveness of this method is shown on two commercial buildings, it can be applied to any geographical scope from regional to national scales, making it a multi-scale model. The proposed model is markedly practical to the policymakers, who can design policies to incentivize GCPVS owners to operate their system for maximum peak load shaving, thereby increasing the overall economic efficiency of the power system.

1. Introduction

The historic 2015 Paris climate agreement aims to limit average global temperature rise to well below 2 °C compared to pre-industrial levels. The decarbonization of the power system will play a major role in achieving this goal as it is a significant source of greenhouse gas (GHG) emissions. To decarbonize the power system, it is widely accepted that a transition from a traditional fossil fuel-based electricity generation system to one based on renewable energy generation is needed [1]. Renewable energy sources such as wind and solar offer abundant and GHG-emission free alternatives to fossil fuels. Among these, solar energy has gained particular attention due to its vast potential [2]. One such technology to harness this vast solar potential is photovoltaic cells, which can be connected to the grid through an inverter, hence referred to as grid-connected photovoltaic systems (GCPVS) [3]. The deployment of GCPVS has been phenomenal in recent years [4,5] due to its various benefits for users and distribution system

operators [6,7]. These benefits, among others, include simple installation and use [8], low maintenance and repair costs [9], capacity to reduce peak loads during hot summer noon [10], reduced losses in transmission and distribution systems [11], and contribution to clean energy production [12,13].

Power generation from photovoltaics (PV) is by nature intermittent due to fluctuations in weather conditions. Also, the orientation of PV modules directly impacts the output power of a GCPVS. Tilt and azimuth angles determine this orientation, which is crucial to the efficiency of PV generation [14]. Varying tilt angle (β) can shift the production from summer months to winter months, while the variation of the azimuth (ψ) from east to west can partly shift daily production between the morning or afternoon hours [15]. Generally, there are two main design architectures for PV installation depending on whether the tilt and/or azimuth can be dynamically adjusted during operation: fixed and movable structures. In fixed structures, as the name implies, PV modules are installed in a fixed and static orientation. These structures are generally positioned to maximize annual electricity generation (i.e., the maximum

E-mail address: reza.bakhshi@tudelft.nl (R. Bakhshi-Jafarabadi).

^{*} Corresponding author.

Nomenclature		P_{MPP}	PV module's MPP power
		h	Hour number over a year
Abbrevia	Abbreviations		Hours with peak load
BESS	Battery energy storage system	$Loss_{cab}$	DC and AC cables' losses
FiT	Feed-in tariff	$P_{inv,ac}$	AC output power of grid-tie inverter
GCPVS	Grid-connected photovoltaic system	$P_{inv,loss}$	Grid-tie inverter losses
GHG	Greenhouse Gas	P_{PV}^h	GCPVS generated power at hth
IP	Intellectual property	P_L^h	Load power at <i>h</i> th
MPP	Maximum power point	S_d^h	Direct solar radiation on a PV surface at <i>h</i> th
NOCT	Nominal operating cell temperature	$\mathcal{S}^h_{PV,d}$	PV module received direct irradiance at <i>h</i> th
NREL	National Renewable Energy Laboratory	T_A	Ambient temperature
PV	Photovoltaic	T_C	Cell temperature
STC	Standard test condition	$T_{C.NOCT}$	Cell temperature at NOCT
Daramet	ers and variables	$T_{C,NOCI}$ $T_{C,STC}$	Cell temperature at STC
C^h	Cost of load energy at hth hour	V_{OC}	PV module's open-circuit voltage
G	PV module's received irradiance	$V_{OC,NOCT}$	
G_{NOCT}	PV module's received irradiance at NOCT	$V_{OC,STC}$	V_{OC} at STC
G_{NOCT} G_{STC}	PV module's received irradiance at NOC1 PV module's received irradiance at STC	α	Sun elevation angle
i i	Sun incident angle	β	PV module's tilt angle
I_{SC}	PV module's short-circuit current	θ	Sun azimuth angle
	I_{SC} at NOCT	ψ	PV module's azimuth angle
I _{SC,NOCT}	I_{SC} at NOC1	$\mu_{I_{SC}}$	Temperate coefficient of I_{SC}
$I_{SC,STC}$ $Loss_{cab}$	Cable losses	γ·1 _{SC} ΥMPP	Temperate coefficient of P_{MPP}
cub	Maximum power, aimed to be shaved	/ WIFF	Tomporate coefficient of 1 wirr
$P_{\rm max}$	maximum power, aimed to be shaved		

yield), as shown in Fig. 1 (a). However, such structures are inflexible in operation and if not optimally oriented during installation, the full potential yield and economic value will be underexploited. On the other hand, movable structures are more dynamic, allowing for variations in the orientation of PV modules by changing the tilt and azimuth angles with respect to fluctuations in solar irradiance. Depending on which plane the PV module can move (i.e., vertical and/or horizontal), three types of configurations exist as shown in Fig. 1 (b), (c), and (d): vertical single-axis tracker, horizontal single-axis tracker, and dual-axis tracker, respectively [16]. In a vertical tracker, the azimuth angle of a PV module is varied with respect to the sun's azimuth. This configuration maximizes short-term production by taking advantage of diurnal and synoptic fluctuations. In a horizontal single-axis tracker, the tilt angle of the PV module varies concerning the sun's elevation. This shifts production between summer and winter, to absorb seasonal fluctuations. Finally, in the dual-axis tracker configuration, the PV module follows the sun's daily and seasonal trajectory, ensuring maximum energy production at all times throughout the year.

Due to the importance of PV orientation in its power production, a vast number of studies have been conducted to determine the optimal orientation (tilt and azimuth angles) of PV modules for both fixed and movable structures. The authors in Ref. [2] experimentally studied how varying tilt and azimuth angles affect PV panel performance, measuring solar radiation, power output, voltage, and current. They found that for Konya, Türkiye, the optimal tilt angle is 32.08° with an azimuth of 0° , highlighting the strong influence of panel positioning on energy generation. For sun trackers, Bahrami et al., [17] focused on optimizing the tilt and azimuth angles of vertical, horizontal, and dual-axis structures for maximum annual received radiation in Europe and Africa. The authors found that the tracking performance closely depends on the locations. Also, the full tracking leads to at most 31.2% and 23.4% more energy, compared with fixed installation with optimum orientation and single-axis tracker, respectively. Note that most movable structures cannot fully track the sun due to mechanical constraints. Mansour et al., [18] developed a mathematical model to optimize the tilt angle of a horizontal-axis tracker for maximum energy yield in Saudi Arabia. The authors concluded that for monthly variations in tilt angles between 20°

and 33°, a 4.2% gain in energy yield is achieved compared to a yearly adjustment. Similarly, Soulayman and Hammoud [19] optimized the tilt of a horizontal vertical-axis movable structure for maximum energy yield in mid-latitude areas. The outputs imply that the average energy gain for daily, monthly, seasonally, and half-yearly adjustments is approximately constant. A plethora of similar studies that optimize tilt and/or azimuth for movable structures under different objectives can be found in the literature, such as profit maximization from the wholesale market [15], cost minimization under electricity and grid tariffs [20], minimum loss of load probability [21], and minimum levelized cost of electricity with investment in GCPVS capacity [22]. Interestingly, the authors in Ref. [23] proposed an alternative approach to boost energy yield by optimizing tilt and solar reflector orientation. They found that annual energy gains could reach 28-31% across 20°-30°N latitudes, with optimal PV tilts between 32° and 40° and reflector tilts between 19° and 13°, recommending just two tilt adjustments per year for practical operation. The authors refer the readers to Ref. [24] for a comprehensive review of such studies and their findings.

Despite the greater potential of energy generation, movable structures require high operational and maintenance costs [16]. Also, these structures suffer from several limitations, such as aesthetics, more shading with the same distance between rows, and a limited range of tracking for constantly adjusting the PV modules to the ideal orientation [25,26]. Moreover, Lv Yuexia et al. suggest that from a practical point of view, it is not advisable to constantly adjust the orientation of PV modules because there is no significance change in total solar energy gains during the sunny season [26]. In such cases, from an economic standpoint, the extra gains in solar generation might not offset the additional operational and maintenance costs incurred in constantly adjusting movable structures. Therefore, some studies have proposed different methods and models to determine the optimal tilt and azimuth angles for fixed structures. For example, an empirical method has been adopted to optimize the tilt angle in Abu Dhabi to maximize annual energy yield [25]. The authors found the yearly optimum tilt to be 20° and suggested that PV modules should be fixed to the latitude of Abu Dhabi. In Ref. [27], Le Roux used measured data from nine solar measuring stations across South Africa to calculate the annual solar

insolation on fixed collectors at all possible installation angles. The author found that the optimum fixed β is similar to the location's latitude and the optimum fixed ψ is a function of the longitude angle minus the absolute latitude angle. At this angle, a fixed installation can on average, collect 10% more annual solar insolation than a horizontally-fixed collector. In Ref. [28], the authors used multi-year ERA5 solar radiation data to optimize fixed tilt angles for PV systems across China, finding that optimized angles can vary by up to 10° depending on the time period and that latitude-based schemes could lead to over 1 TWh/year in PV power losses. Their results emphasize the need for long-term, region-specific, and data-driven optimization to maximize solar yields. In Ref. [10], the authors optimized tilt and azimuth for maximum self-consumption in 90 buildings in the Netherlands. The outputs indicate that maximum self-consumption can be achieved for a fixed structure with $\psi = 212^{\circ}$ and $\beta = 26^{\circ}$. In Ref. [29], Shekar et al. analyzed the impact of PV azimuth angle on maximum energy yield and the economic value in terms of levelized cost of energy. Their results showed optimal azimuth ranges of 70°-270° at a 3% discount rate and 120°-200° at a 5% discount rate, with an economic optimum at 156°. Rhodes et al. optimized the orientation of a fixed structure in the USA under multiple objectives, such as maximum annual yield and the economic value of electricity in the wholesale market [30]. They found that a few degrees towards the horizontal (from the rule of thumb 30°) might be a better tilt for energy production, and the optimal azimuth was pushed further west $(20^{\circ}-51^{\circ})$ based on the wholesale market value of electricity. In Ref. [31], the authors determined the optimum orientation for maximizing revenues from electricity sales in Canada. The results indicate that the optimal tilt angle is between 32° and 38° while the optimum azimuth is in the range of 1°W-6°E. Many similar studies that optimized the tilt and azimuth of fixed structures can be found in the literature under various objectives such as costs/revenues minimization/maximization from electricity consumption/generation [32], cost minimization under different feed-in-tariff (FiT) [33], and the minimization of levelized cost of electricity considering investment in the power capacity of the GCPVS [34].

Another important, perhaps most crucial application of GCPVS from a system-wide perspective is to operate them for peak load shaving in the power system. Reducing the demand for electrical power in peak periods economically benefits both the system operator and customers. Reduction in peak power flows mitigates the need for investment in network upgrades for the system operator and eliminates the need to dispatch expensive marginal generators, increasing the economic efficiency of the power system. Therefore, another category of studies has focused on optimizing GCPVS capacity (sometimes coupled with BESS) or their operation management strategies for maximum peak load shaving. For instance, Ceran et al., [35] developed a mathematical

model to analyze the impact of national peak load shaving with GCPVS installed in office buildings in Poland. They found that the highest peak load shaving at the country level is 200 MW, with an aggregated office building PV capacity of 273.75 MWp (with a southeast orientation). Yanxue et al. developed a simulation model to investigate the impact of different management strategies on the peak load shaving potential of GCPVS in Japan [36]. They concluded that if the PV-battery system of all homes accounts for only 2% of the grid load, then such a system can reduce peak load by 1.1%, demonstrating its potential to provide grid-supporting services. Similar studies have been conducted at different scales and geographical regions, including Costa Rica [37], Iran [38], and the Netherlands [39].

A summary of our comprehensive literature review is provided in Table 1. As can be seen, several gaps still exist in the current literature. First, several papers have optimized tilt and azimuth angles to maximize either annual received radiation and energy yield (self-consumption) and/or minimize the electricity costs, while a few studies have optimized GCPVS capacity (in combination with BESS) for peak load shaving. However, none of these studies optimized the tilt and azimuth angles of fixed structure GCPVS for maximum peak load shaving. As mentioned earlier, this optimization reduces the need to over-design the power system and accordingly, the required investment in grid upgrades. Since the whole/partial costs of grid upgrades would be passed to the end users, the proposed optimization leads to a higher cost efficiency. Second, most peak load shaving and optimization of the PV orientation have been formulated for a specific project and geographical location, limiting their application range. Last but not least, the outputs of such studies rely highly on the precise modeling of the components. As another research gap, several works lack accuracy for the employed model, e.g., disregarding the efficiency model for the components or considering the fixed efficiency for PV module/inverter/etc. irrespective of the GCPVS's operating points. To fill the aforementioned gaps, this paper proposes a multi-scale search-based optimization algorithm to determine the tilt and azimuth angles of a fixed structure for maximum peak load shaving. The method is built upon eminently precise modeling for GCPVS's components to ensure the reliability of the results. Also, the proposed work is a multi-scale model (from household to regional and national scales) and can be adopted for any PV technologies and geographical sites. In sum, the main contributions of the proposed work include:

 To our best knowledge, tilt and azimuth angles of the fixed structure are optimally determined for the first time to reach the maximum peak load shaving, reducing the costs of the grid upgrades which enhances the cost efficiency for end users.

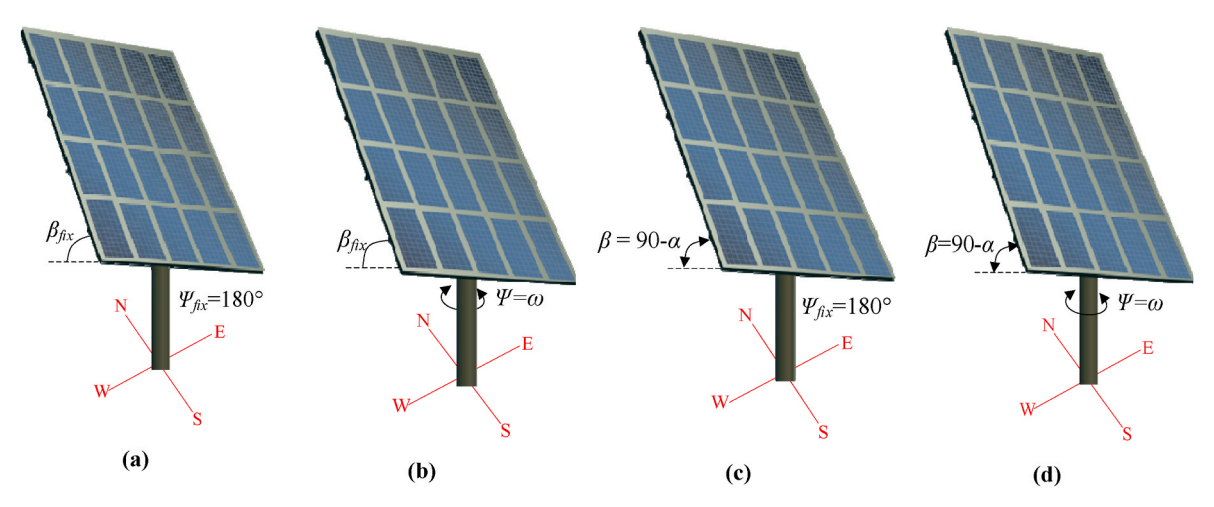


Fig. 1. PV module structures in a northern hemisphere: a) Fixed, b) Vertical single-axis tracker, c) Horizontal single-axis tracker, d) Dual-axis tracker.

Table 1Summary of relevant literature investigating GCPVS structure/size optimization.

Reference	Studied system	GCPVS structure Type	Objective for optimizing GCPVS orientation and inclination angles	Application scope	Model's accuracy?
[15]	GCPVS	Movable structure	Maximize annual energy yield	Large scale	Low ^b
[17]	GCPVS	Movable structure	Maximize annual received radiation	Multi-scale	N/A ^a
[26]	GCPVS	Fixed structure	Maximize self-consumption	Multi-scale	Low ^b
[25]	GCPVS	Fixed structure	Maximize annual received radiation	Multi-scale	N/A
[18]	GCPVS	Movable structure	Maximize annual energy yield	Residential	Moderate ^b
[27]	GCPVS	Fixed structure	Maximize annual yield	Buildings' rooftop	High
[31]	GCPVS	Fixed structure	Minimize electricity cost	Small scale	High
[30]	GCPVS	Fixed structure	Minimize electricity cost	Large scale	Moderate ^c
[33]	GCPVS	Fixed structure	Maximize electricity revenues	Large scale	Low ^b
[32]	GCPVS	Fixed structure	Maximize electricity revenues	Large scale	Low ^b
[22]	GCPVS	Movable structure	Minimize electricity cost	Large scale	Low ^c
[34]	GCPVS-BESS	Fixed structure	Minimize electricity cost	Small scale	Low ^c
[35]	GCPVS-BESS	Fixed structure	×	Large scale	Moderate ^b
[37]	GCPVS-BESS	Fixed structure	×	Small scale	Low ^{b,c}
[38]	GCPVS-BESS	Fixed structure	×	Small scale	High
[39]	GCPVS-BESS	Fixed structure	×	Small scale	High
[19]	GCPVS	Movable structure	Maximize annual received radiation	Multi-scale	N/A
[40]	GCPVS	Fixed structure	×	Small scale	High
Proposed work	GCPVS	Fixed structure	Maximize peak load shaving	Multi-scale	High

- ^a Study focuses on radiation modeling and not the GCPVS energy generation.
- ^b Neglecting the precise model for PV module, inverter, etc. in the methodology.
- ^c Considering fixed efficiencies for some/all components in the analysis.
- The proposed methodology is structured for all GCPVS technologies and ratings and does not depend on the site and load profile. Thus, it covers all peak load shaving applications of GCPVS, from household and commercial buildings to regional and national scales.
- The conversion of solar irradiance to AC power is performed with accurate physics models, ensuring the reliability of the results.
- Findings are valuable to policymakers to revise the incentive policies toward ensuring the GCPVS owner's profit with optimum peak load shaving installation, e.g., multi-level FiT.

The remainder of this article is organized as follows. Section 2 provides a detailed description of the methodology, including the mathematical optimization model and energy determination process. Then, Section 3 presents the simulation and optimization results for two case studies in Delft and Mashhad. Section 4 discusses the proposed method and lays the foundation for future research. Finally, the concluding remarks are elucidated on Section 5.

2. Methodology description

This section describes the mathematical formulation of the optimum peak load shaving problem, the PV output calculation model, and the implementation of the proposed solution algorithm.

2.1. Optimum peak load shaving formulation

This paper optimizes the tilt and azimuth angles of a fixed structure for maximum peak load shaving. In literature, tilt and azimuth angles have been optimized for different techno-economic objectives, such as maximum annual generated energy, maximum profit in FiT scheme, and minimum load support from the grid. These goals can be formulated as follows:

$$Max f(\beta, \psi) = \sum_{h} P_{pV}^{h} \tag{1}$$

$$Max f(\beta, \psi) = \sum_{h} FiT^{h}P_{PV}^{h}$$
 (2)

$$Max f(\beta, \psi) = \sum_{h} C^{h} \left(P_{PV}^{h} - P_{L}^{h} \right) \tag{3}$$

where, P_{PV}^h and P_L^h are the power of GCPVS and load within h^{th} hour,

respectively. Also, C^h and FiT^h represent the electricity cost and FiT at h^{th} hour, respectively. Note that under a fixed FiT policy ($FiT^h = FiT$), the results of Eqs. (2) and (3) would be the same. Also, the first two objective functions do not rely on local load profile, while it affects the optimization in Eq. (3), minimizing the electricity bills.

This paper introduces the peak load shaving objective function for the first time, aiming to maximize supporting the load within the peak hours (h_i):

$$Max f(\beta, \psi) = \sum_{h \in h} (P_{PV}^h - P_L^h) \quad \text{where } h_i : P_L^{h_i} \ge P_{\text{max}}$$
 (4)

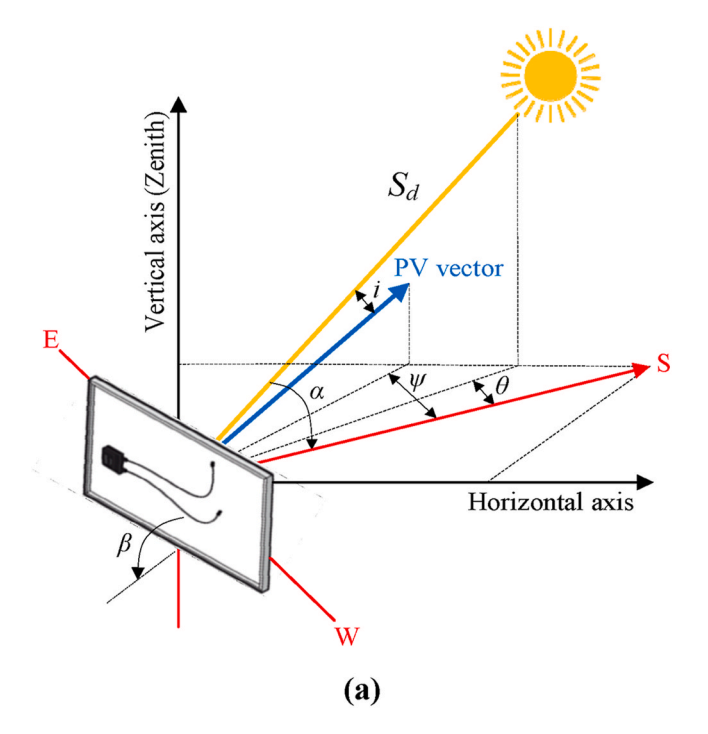
Above equations can be combined in a single objective function as follows:

$$\begin{aligned} \textit{Max}\, f(\beta, \psi) &= \left(x_1 \sum_h P_{PV}^h\right) + \left(x_2 \sum_h FiT^h P_{PV}^h\right) + \left(x_3 \sum_h C^h \left(P_{PV}^h - P_L^h\right)\right) \\ &+ \left(x_4 \sum_{h \in h_i} \left(P_{PV}^h - P_L^h\right)\right) \quad \textit{where} \ \ h_i \\ &: P_L^{h_i} \geq P_{\max} \end{aligned}$$

In the recent expression, x_1 , x_2 , x_3 , and x_4 are binary parameters subject to the constraint: $x_1+x_2+x_3+x_4=1$. This constraint allows the designer to choose the right objective function regarding the tilt and azimuth optimization goal and existing incentive (if any). As explained, the first term $(x_1=1)$ leads to an optimization for maximum annual yield of GCPVS. The second and third terms find optimum angles under the existing FiT scheme and net metering policies, i.e., $x_2=1$ and $x_3=1$, respectively. The last term, the new objective function introduced in this paper, determines the optimum tilt and azimuth for maximum peak load shaving $(x_4=1)$. Thus, the focus is to shave the peak load within the time intervals (h_i) where demand is greater than a maximum level (P_{max}) , i.e., the algorithm finds the optimal values for β and ψ to limit P_L to P_{max} as much as possible.

2.2. PV output calculation model

The PV output and energy calculation model show the effect of β and ψ in the maximum peak load shaving formulation. According to Fig. 2, the received direct irradiance of the fixed structure $(S_{PV,d}^h)$ can be quantified in the zenith vs. horizontal plane based on the extraterrestrial



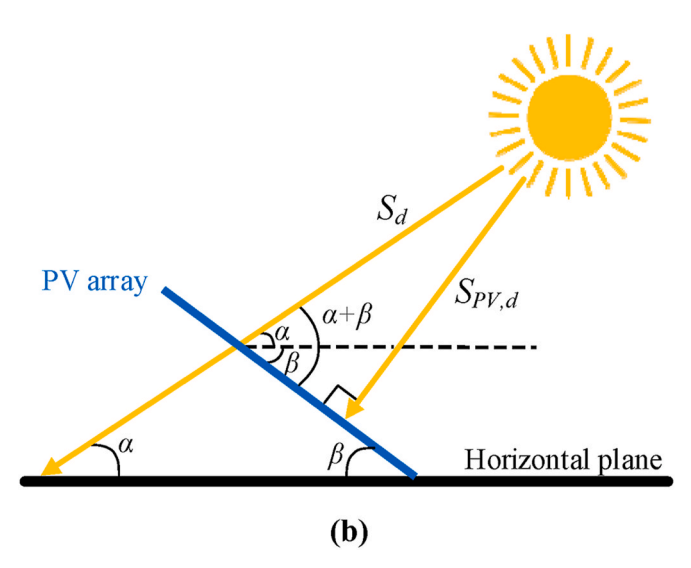


Fig. 2. Solar radiation formulation: a) Schematic illustration of a PV module and solar irradiance angles, b) Incident reflection on PV vector.

direct solar radiation on a PV module (S_d) :

$$S_{PV,d}^{h} = S_{d}^{h} \times \cos(i) = S_{d}^{h} \times [\cos \alpha \sin \beta \cos(\psi - \theta) + \cos \beta \sin \alpha]$$
 (6)

where, i is the incident angle as shown in Fig. 2 (a). Also, θ and α represent sun azimuth and elevation angles, respectively. According to the reflection of the incident on the PV vector, β and ψ determine the received solar irradiance (Fig. 2 (b)). This can be explained for different structures; the sun's east-to-west trajectory (reflected by β) and south-to-north trajectory (reflected by ψ) are tracked in vertical and horizontal single-axis structures, respectively. The dual-axis structure tracks the sun in both directions, i.e., β and ψ are dynamically changed over time. Finally, β and ψ are both constant in a fixed structure. This paper proposes finding these angles for the first time to reach maximum peak shaving, i.e., Eq. (5) under $x_1 = x_2 = x_3 = 0$ and $x_4 = 1$. To this end, a high-fidelity model for GCPVS components is used to calculate the annual energy yield, as detailed in Fig. 3. The method involves

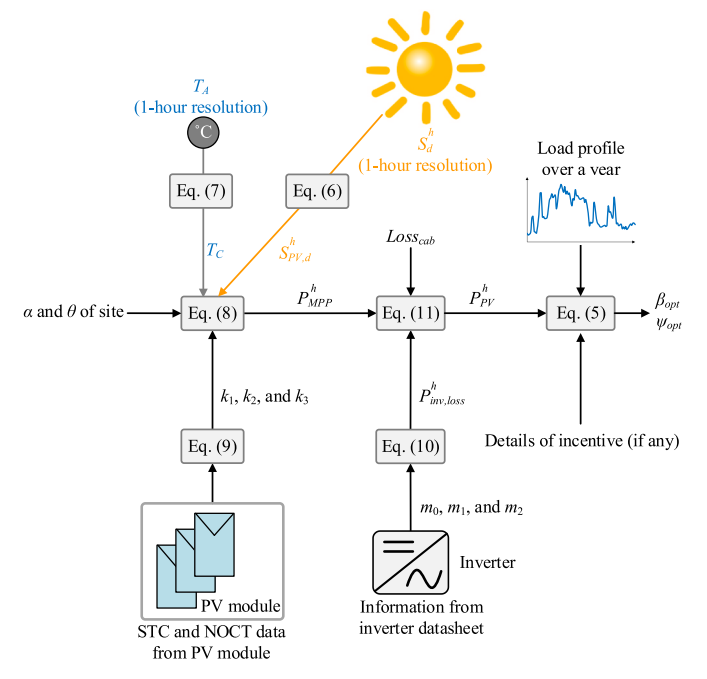


Fig. 3. Detailed flowchart of the proposed optimization approach.

meteorological measurement as well as PV module's and inverter's datasheet in the energy calculation process. Among various meteorological factors that affect the GCPVS output, received irradiance and cell temperature are two main ones. Thus, the performance of PV module under various cell temperatures and irradiance levels is given by all manufacturers.

The GCPVS energy calculation process initiates by transforming the field measurement of the irradiance into the received one at PV module surface. To this end, a 1-h extraterrestrial direct solar irradiance is taken from existing resources, e.g., the National Renewable Energy Laboratory [41], PVGIS [42], and Solcast databases [43]. Then, Eq. (6) determines the received solar irradiance of the fixed structure for various β and ψ , considering α and θ of the site.

As noted earlier, another important variable in determining the power output of GCPVS is the cell temperature (T_C). Since ambient temperature (T_A) is mainly recorded instead of T_C , following expression is used. This term finds T_C from T_A , considering G which is the received solar incident (W/m^2):

$$T_C = T_A + \left(\frac{T_{C,NOCT} - 20}{0.8}\right) \frac{G}{G_{STC}} \tag{7}$$

where, $T_{C,NOCT}$ stands for the cell temperature (°C) at nominal operating cell temperature (NOCT) condition with 20 °C and 800 W/m² [44]. Also, G_{STC} is the received irradiance in standard test condition (STC) and equals 1000 W/m². In STC, the cell temperature ($T_{C,STC}$) and air mass are 25 °C and 1.5, respectively.

The current, voltage, and power of the PV module at maximum power point (MPP) operation can be computed accordingly through the estimated radiation and temperature based on the following model [45]:

$$\begin{cases} I_{MPP} = I_{MPP,STC} \times \left[1 + \mu_{I_{SC}} (T_C - T_{C,STC})\right] \left(\frac{G}{G_{STC}}\right)^{k_1} \\ V_{MPP} = \frac{V_{MPP,STC}}{1 + k_2 \ln \left(\frac{G}{G_{STC}}\right)} \left(\frac{T_{C,STC}}{T_C}\right)^{k_3} \\ P_{MPP} = P_{MPP,ref} \frac{G}{G_{ref}} \left[1 + \gamma_{MPP} (T_C - T_{ref})\right] \end{cases}$$

$$(8)$$

where, $\mu_{I_{SC}}$ and γ_{MPP} are the temperature coefficient of the PV module's short-circuit current (I_{SC}) and MPP power (P_{MPP}), respectively. These data are available in the PV module's datasheet, presented by the manufacturer. Furthermore, k_1 to k_3 are the model coefficients that should be defined through the following equations, using two arbitrary operating points, e.g., NOCT and STC. It is worth mentioning that the vendor presents these voltage and current data in the PV module's datasheet.

$$\begin{cases} k_{1} = \frac{\ln(I_{SC_{STC}} - \mu_{I_{SC}}(T_{STC} - T_{NOCT})/I_{SC_{NOCT}})}{\ln(G_{STC}/G_{NOCT})} \\ k_{2} = \frac{(V_{OC_{NOCT}}/V_{OC_{STC}}) - 1}{\ln(G_{NOCT}/G_{STC})} \\ k_{3} = \frac{\ln(V_{OC_{NOCT}}/V_{OC_{STC}})}{\ln(T_{STC}/T_{NOCT})} \end{cases}$$
(9)

where, V_{OC} is the PV module's open-circuit voltage. Also, subscripts "STC" and "NOCT" denote the variables at STC and NOCT operations, respectively. Note that although this paper formulates the equations for mono-facial solar modules, the presented methodology/equations can be simply reformulated to bi-facial ones.

The grid-tie inverter losses are calculated after computing the PV module output power. For a high-fidelity precise model, Rampinellia et al. proposed the following polynomial expression to estimate the inverter losses ($P_{inv, loss}$) [46]:

$$P_{inv,loss} = m_0 + m_1 P_{inv,ac} + m_2 P_{inv,ac}^2$$
 (10)

where, m_0 , m_1 , and m_2 are defined through the curve fitting approach, using several levels of the AC output power of the inverter ($P_{inv,ac}$). Similarly, these data are given by the inverter manufacturer.

Finally, the output power can be precisely determined by considering the cable losses ($Loss_{cab}$) as follows:

$$P_{PV} = P_{MPP} \times \left(1 - P_{inv,loss}\right) \times \left(1 - Loss_{cab}\right) \tag{11}$$

According to Eqs. (6)–(11), P_{PV} relies on both field measurement (to determine G and T_C) and GCPVS characteristics (to quantify the output power and exiting losses). High resolution of the first data is available in several resources, while for the latter, this paper exploits high accurate models for PV module and inverter.

The P_{PV} variable in Eq. (5) can be replaced by the expression in Eq. (11) to determine the peak load shaving for various azimuth and tilt angles. In this work, the analysis is performed over a year. In our proposed search-based optimization algorithm, the β and ψ with the greatest fitness function under $x_4=1$ are chosen as the optimum solution.

2.3. Solution algorithm

The flowchart of the proposed search-based solution algorithm is depicted in Fig. 4. From the realization perspective, the algorithm includes two main stages: the initialization and optimum result(s) search. In the initialization stage, the GCPVS characteristics and site data are imported into the model. The system configuration and size, components, and electrical design are set to their assumed predefined values at this stage. The inputs of the initialization procedure include:

- Site meteo data over a year, including solar irradiance and temperature.
- The system details, including components' characteristics, numbers, and electrical design. It is assumed that the number of PV modules in series and parallel strings is defined respecting the electrical design limitations [3].
- Local load profile over a year, aimed to be shaved optimally.

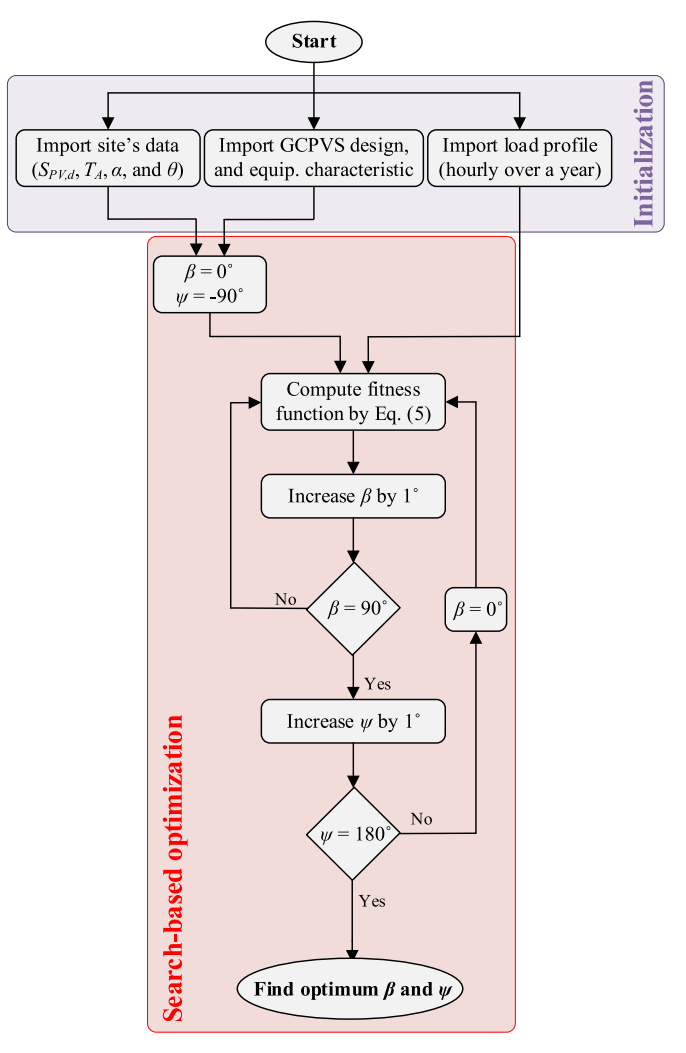


Fig. 4. Flowchart of the proposed search-based optimization methodology.

Details of the site's electricity rate and incentive policy (if any), i.e.,
 FiT^h and C^h in Eq. (5).

As shown in Fig. 3, the first two data sets are used to determine the GCPVS's hourly energy generation over a year. Disregarding the selected objective function, the GCPVS's power should be computed. The load profile can be used to maximize the peak load shaving or minimize the electricity bills. The last data is solely used for additional analysis, evaluating the peak load shaving for β and ψ corresponding to the optimum solution under existing policies. The summary of the used data for each objective function is tabulated in Table 2.

After computing P_{PV}^h , the optimal values of β and ψ can be found using the selected objective function, e.g., by setting $x_4=1$ in Eq. (5) for maximum peak load shaving. The load profile of the studied case is exploited to determine the objective function for each selected set of solution. Therefore, it markedly influences the optimum solutions as shown later for two different case studies. The β and ψ with the highest fitness function value are chosen as the optimum solution. These variables are searched over the feasible range, i.e., $\beta = [0^{\circ}, 90^{\circ}]$ and $\psi = [-90^{\circ}, 90^{\circ}]$ in the northern hemisphere. Hence, the number of scenarios depends on the chosen step for β and ψ . This step should be defined as a trade-off between computational requirements and the result's accuracy, i.e., a larger step reduces the computational time and the accuracy/optimality of the solution. In this paper, a 1° step is chosen, resulting in 90 × 180 = 16,200 cases. Since this computational process is still heavy, several suggestions are provided later to mitigate the computational time.

It is worth mentioning that a practical application of this work is policymakers such as distribution and transmission system operators. As shown later, they can use the output of such optimization to design policy incentives that maximize economic benefits for the investors when they operate their systems to align with peak load reduction. Also, the formulations above can be applied to all GCPVS (rooftop and ground-mounted at all scales) and loads (household and industrial), covering a wide range of applications.

3. Simulation results

3.1. Case studies description

The proposed optimization is performed for two commercial buildings in Delft, the Netherlands (52.0116° N, 4.3571° E) and Mashhad, Iran (36.2972° N, 59.6067° E). The peak load is challenging in Iran at noon during the summer due to the deployment of air conditioning systems. The Ministry of Energy established a FiT framework for private and government-based individuals, detailed in Ref. [47]. The FiT relies on the GCPVS nominal power, e.g., $0.039 \, \text{€/kWh}$ for all GCPVSs smaller than 20 kW. In the Netherlands, however, the peak load occurs in cold afternoons as heating systems are used. The Dutch government legalized the net metering policy for buildings to reduce electricity bills. The electricity price varies in peak (7 a.m.–9 p.m.) and non-peak hours every season. The rates in peak hours are 0.424, 0.377, 0.396 and 0.395 €/kWh, and 0.420, 0.376, 0.390 and 0.392 €/kWh during non-peak hours of spring, summer, autumn, and winter. These values will be used later to optimize the tilt and azimuth angles under net metering policy.

According to the method's flowchart, the optimization starts with importing the data, i.e., the initialization. The sites' data and one-year hourly load profile are imported for Mashhad [48] and Delft [49]. As explained later, the existing data have been re-scaled according to the solar potential of the sites. Also, $P_{\rm max}$ in Eq. (5) is set at 5 kW; thus, h_i includes the hours that P_L exceeds 5 kW.

The optimization is conducted in both cities for a 10 kW GCPVS, shown in Fig. 5. This GCPVS includes two strings connected to the inverter's MPPs to ensure the electrical design limitations [47]. The PV strings and inverter are protected against overcurrent and abnormal voltage through DC and AC enclosures, respectively. According to the existing policy, the GCPVS owner can benefit from net metering and FiT, displayed by orange and blue paths in Fig. 5.

3.2. Optimization results for delft

The site, GCPVS, and load data are imported based on the proposed methodology structure. The hourly load data in 2023 are obtained from Ref. [49], category E1A, representing the Dutch demand for household and commercial buildings in a low-voltage distribution grid. This normalized load is modified so that the peak load equals 8 kW. The GCPVS attempts to shave the load greater than 5 kW ($P_{\rm max}=5$ kW). Solar irradiance and temperature data are also taken from Refs. [42,50]. In addition, solar module and inverter are modeled using their datasheet

Table 2Inputs and implementation of the algorithm for different objective functions.

Optimization target	Implementation in Eq. (5)			in	Data used		
	x_1	<i>x</i> ₂	x_3	<i>x</i> ₄	Site's data	Load profile	Incentive (if any)
Max. annual yield	1	0	0	0	✓	×	×
Max. profit under FiT	0	1	0	0	✓	×	1
Min. electricity bills	0	0	1	0	✓	✓	×
Max. peak load shaving	0	0	0	1	1	✓	1

information. Finally, *Loss_{cab}* is considered 2%, similar to Ref. [3]. The details of the GCPVS model and supportive policy are listed in Table 3.

Figs. 6 and 7 present the simulation results for Delft. The tilt and azimuth angles are initially modified to find the optimum ones for maximum annual generated energy. The energy is at most 10,893 kW/year for $\beta=41^\circ$ and $\psi=0^\circ$. This confirms the results obtained in the literature, i.e., maximum yield can be fulfilled when β is close to the location's latitude and PV is facing the south for the northern hemisphere [25,27]. Also, Fig. 6 (a) shows the effect of tilt and azimuth on the annual generated energy. The areas encompassed by the red, blue, and black lines imply β and ψ with, respectively, 2%, 5%, and 10% energy drop compared to the optimum solution. When $\beta=60^\circ$, for example, the annual energy is 90% of the maximum level for $-41.5^\circ \leq \psi \leq 41.5^\circ$.

When the goal is to reduce the electricity bills ($x_3=1$ in Eq. (5)), the GCPVS power should align with the costly load. However, the electricity cost of peak loads barely affects the annual electricity bill minimization due to two reasons: the electricity rates in peak and off-peak hours are almost the same, and peak hours are defined as 7 a.m. to 9 p.m. for all days in the Netherlands, i.e., GCPVS generation coincides with the peak hours. The simulation results are presented for several tilt and azimuth angles in Fig. 6 (b). The outputs reveal that the electricity bills are minimum (8277.36 €) for $\beta=40^\circ$ and $\psi=0^\circ$. Since the GCPVS produces mainly within the peak hours, the result is close to the maximum annual yield. Also, the electricity bills are low for a wide range of $-30^\circ \le \psi \le 30^\circ$ and $30^\circ \le \beta \le 50^\circ$.

The optimum tilt and azimuth angles are also determined through the proposed optimization method. Fig. 7 (a) and (b) illustrate the level of peak load shaving for various tilt and azimuth angles. The maximum peak load shaving is achieved by orienting the PV array to the southwest ($\psi=45^{\circ}$) and $\beta=24^{\circ}$, i.e., aligning with the peak loads in the afternoons. Further, the amount of energy during peak hours ($P_L \geq 5$ kW) reduces from 8769 kWh (last gray column in Fig. 7 (c)) to 6801.2 kWh (last orange column in Fig. 7 (c)), indicating 22.4% peak load shaving by GCPVS.

The effect of the proposed method on peak load shaving can be further analyzed by Fig. 7 (d)-(f), illustrating the demand distribution for the Dutch household and commercial buildings without and with GCPVS (for optimum shaving and maximum energy yield cases). In this figure, negative energy demand indicates the cases wherein the GCPVS generated energy is greater than the load consumption for that particular timeframe, which will be considered in the next bills. It is observed that the load is effectively shifted from higher levels to lower ones during the day. This peak shaving occurs especially in the afternoons of winter, orange chart in Fig. 7 (d)-(f). For example, energy demand before GCPVS installation is 5661.4 kWh during 12-15 h. This load is reduced to 884.9 kWh and 449.2 kWh when GCPVS is installed according to the maximum energy yield and maximum peak load shaving, respectively. These results corroborate that although the GCPVS generates less energy with the found optimum orientation than the one with the maximum annual yield, the greatest peak load shaving is achieved.

3.3. Optimization results for mashhad

The methodology is also implemented in Mashhad City, with a semiarid climate. Since the solar potential is significantly higher in Mashhad than in Delft, one year of real data for a commercial building is scaled so that the maximum power is 15 kW. The optimization solutions for maximum profit in the existing FiT policy and peak load shaving are also computed.

Initially, the optimum solution under the FiT scheme ($x_2 = 1$ in Eq. (5)) is found. Since the *FiT* rate is fixed at 0.039 ϵ /kWh for the 10 kW GCPVS in Iran, Eq. (5) can be simplified as follows:

$$Max f(\beta, \psi) = \sum_{h} FiT^{h} P_{PV}^{h} = 0.039 \sum_{h} P_{PV}^{h}$$
 (12)

Therefore, it can be considered as a maximum annual energy yield

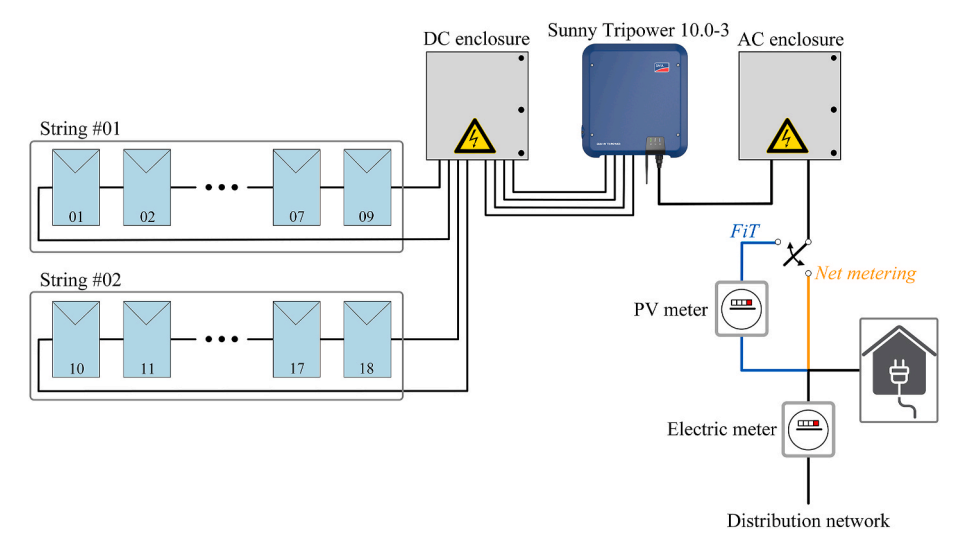


Fig. 5. Layout of the studied 10 kW GCPVS layout.

Table 3Required data for initialization of the proposed method.

GCPVS					
JAM72S30 550 MR PV module		MPP power	550 W		
at STC [01]	MPP voltage	41.96 V		
		MPP current	13.11 A		
		Open-circuit voltage Short-circuit current	49.90 V		
			14.00 A		
		μ_{ISC}	0.045%/°C		
		γ _{MPP}	-0.35%/°C		
		Model parameter k_1 , k_2 ,	1.0113, 0.2892, and		
		and k_3	0.1135		
Inverter [5	2]	No of MPPTs and inputs	MPPT A: 2; MPPT B: 1		
		Max input voltage	1000 V		
		Max input current	MPPT A: 30 A; MPPT		
			B: 18 A		
		MPP voltage range	320-800 V		
		Model parameter m_0 ,	0.0035, 0.0069, and		
		m_1 , and m_2	0.0070		
Cable losse	s	Loss _{cab}	2%		
Location	Renewable energy policy				
Delft	Net metering (2024	rates in €/kWh)			
Peak hours (spring, summer, fall, winter): 0.424, 0.377, 0.396, 0					
Off-peak hours (spring, summer, fall, winter): 0.420, 0.376, 0.390, 0					
Mashhad	FiT (2024 rate in €	/kWh)			
	0.039 €/kWh for GCPVSs <20 kW				
	0.034 €/kWh for GCPVSs <200 kW and >20 kW				

optimization. Similar to the Delft case, the results in Fig. 8 indicate that the annual energy is maximum (16,612 kWh) for $32^\circ \leq \beta \leq 35^\circ$ and $\psi=0^\circ$ (orienting to the South). In this figure, the tilt and azimuth

corresponding to 2%, 5%, and 10% annual yield drop compared to the maximum one are displayed through areas encompassed by black, blue, and red lines. Thus, when installation with the optimum solution is not feasible, e.g., due to shading objectives, it can be mounted within the presented ranges.

Fig. 9 shows the outputs of the peak load shaving optimization for $P_{\rm max}=5$ kW. The effect of tilt and azimuth on peak load shaving is depicted in Fig. 9 (a), where tilt angles with low peak shaving are excluded. According to Fig. 9 (a) and (b), the optimum solution is $\beta=12^{\circ}$ and $\psi=-10^{\circ}$ wherein 4727.4 kWh of the peak load is shaved by GCPVS. This is evident from the last gray and orange columns in Fig. 9 (c); the 10346.9 kWh peak demand is mitigated to 1989.1 kWh. Also, the load distribution in Fig. 9 (d)–(f) corroborates the optimization findings, i.e., the GCPVS effectively supports the load during the day, especially during 8–15 h of summer noon due to the GCPVS's small tilt angle. This shaving is demonstrated by green and red charts in Fig. 9 (d)–(f).

From the analysis, it is concluded that the proposed method can maximize the level of peak load shaving under $x_4 = 1$ in Eq. (5). Even with reduced annual yield (comparing with $x_1 = 1$ in Eq. (5)), this performance is achieved by aligning further the generated energy with the peak load profile. Orienting the solar structure to the optimum solution needs an economic motivation, which is elaborated on later.

4. Discussions and comparison with literature

This section initially compares the outputs of this work with literature and then discusses its practicability (for future implementation), limitations, and potential improvements in future works.

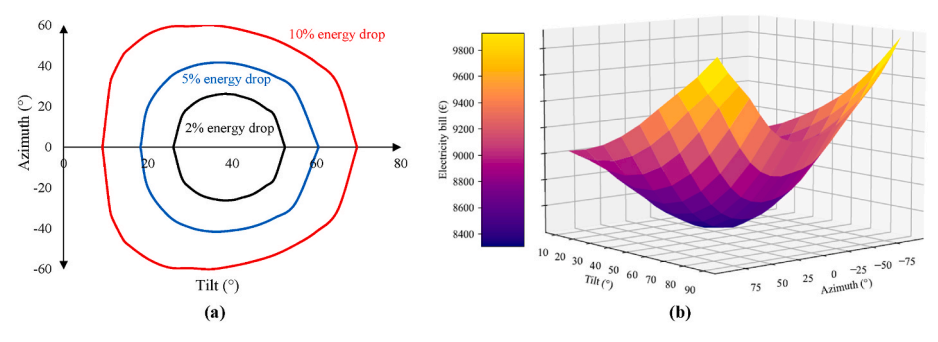


Fig. 6. Simulation results for various tilt and azimuth in Delft City: a) Annual generated energy, b) Annual electricity bills.

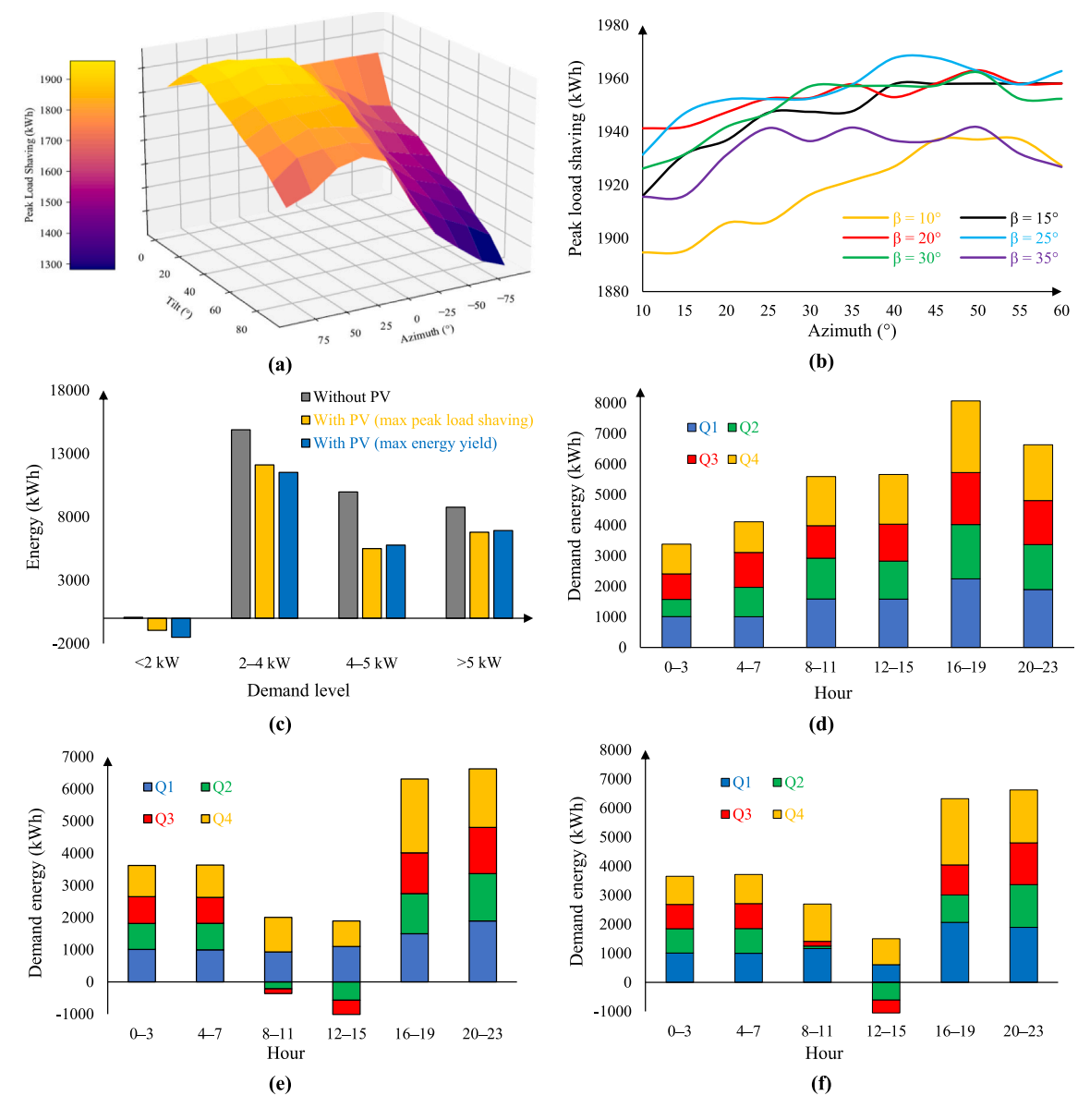


Fig. 7. Simulation results for Delft: a) Peak load shaving for various tilt and azimuth, b) Detailed peak shaving results, c) Load distribution regarding the demand level, d) Load distribution vs. time (with GCPVS), e) Load distribution vs. time (with GCPVS, having max annual yield), f) Load distribution vs. time (with GCPVS, having max peak load shaving).

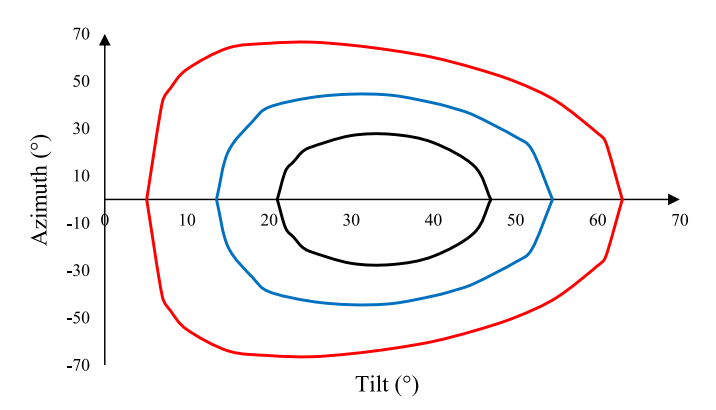


Fig. 8. Simulation results for various tilt and azimuth in Mashhad City.

4.1. Comparsion with literature

This part includes the existing works with only GCPVS and excludes the GCPVS-BESS studies. The logic behind this selection is that the objective function and constraints of GCPVS-BESS are fully different from the current work. In such hybrid applications, the goal is to charge BESS in off-peak and discharge it during peak durations. Similar to Refs. [34–39], the constraints of the optimization include technical limitations of BESS to ensure its long life operation, e.g., keeping the state of charge within a predefined range. From the objective function perspective, the main goal would be to orient the PV module to have maximum generation during off-peak hours. As noted, this is fully different from the objective of the current work, aiming to orient PV modules to have maximum generation during peak load durations.

According to Eq. (5), the optimization of tilt and azimuth of the fixed solar system can be performed for maximum annual yield ($x_1 = 1$), maximum profit under FiT ($x_2 = 1$), minimum electricity bills under net metering ($x_3 = 1$), and peak load shaving ($x_4 = 1$). This paper introduces the last one for the first time and cannot be compared with literature.

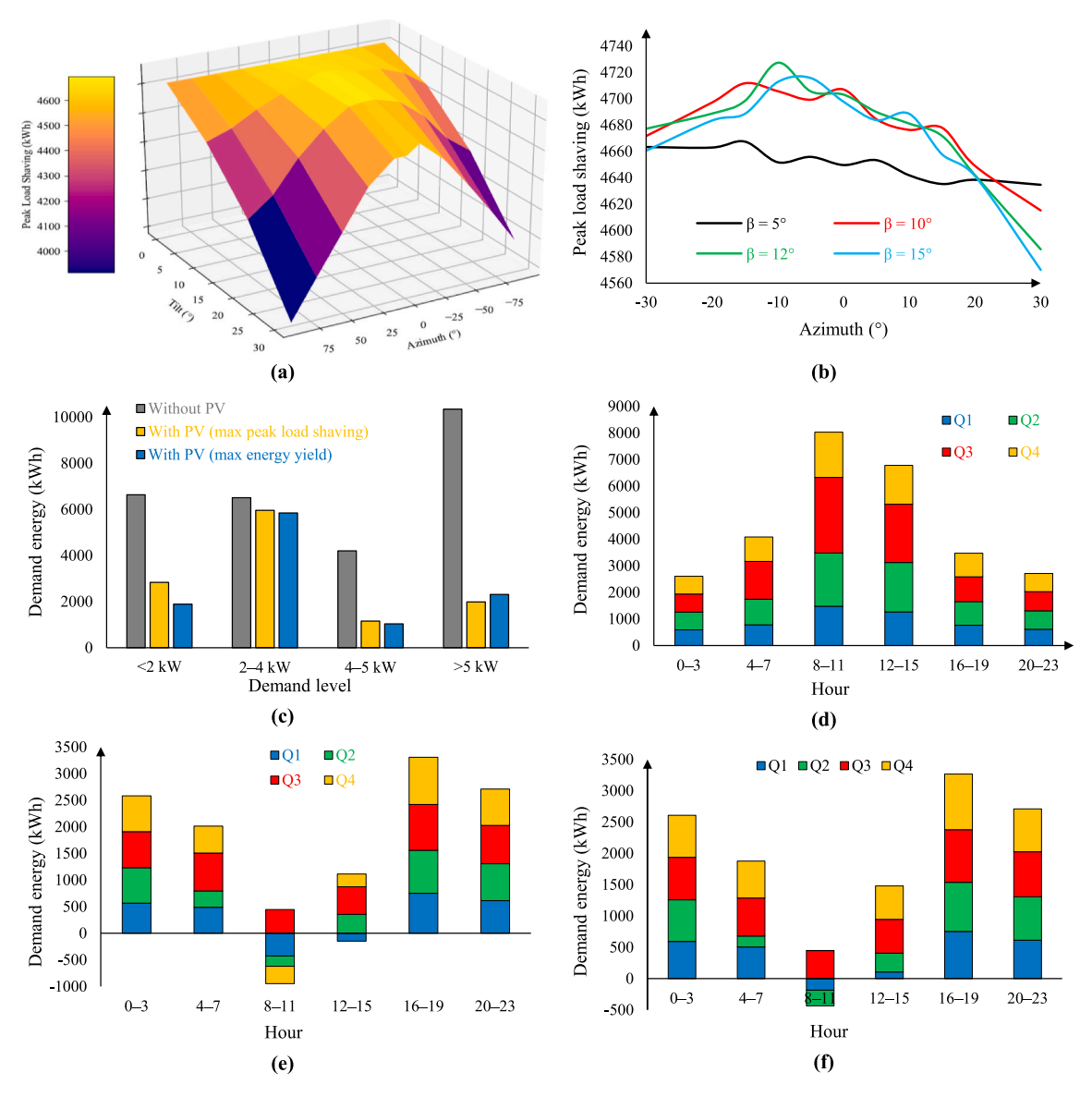


Fig. 9. Analysis for Mashhad City: a) Outputs for maximum peak load shaving, b) Detailed search for maximum peak load shaving, c) Load profile distribution (without/with GCPVS deployment), d) Results for maximum FiT (max energy yield), d) Load distribution regarding the time (without GCPVS), e) Load distribution vs. time (with GCPVS, having max annual yield), f) Load distribution vs. time (with GCPVS, having max peak load shaving).

However, other objective functions can be compared with the results obtained in this work, as summarized in Table 4.

The studies in Refs. [25,27] found that the optimum orientation for maximum annual yield can be fulfilled when tilt is close to the location's latitude and azimuth is a function of the longitude angle minus the absolute latitude angle (i.e., $\psi \sim 0^\circ$ for the northern hemisphere). The obtained results in Fig. 6 (a) and 8 corroborate these findings. In Mashhad with 36.2972 °N, 59.6067 °E, the optimization finds $32^\circ \leq \beta \leq 35^\circ$ and $\psi = 0^\circ$ as the optimum orientation for maximum annual energy. In Delft with 52.0116 °N, 4.3571 °E, the optimum solution is also $\beta = 41^\circ$ and $\psi = 0^\circ$. It is worth noting that not only the optimum solution is found for the two above cities in this paper, but also Fig. 6 (a) and 8 define different ranges of the annual energy yield, e.g., 98%, 95%, and 90% of the optimum solution. The system owner/designer/installer can exploit this practical information in cases where not all orientations are feasible. To this end, the feasible solution(s) with the maximum annual yield is chosen.

The optimum orientation of the fixed solar system for minimum electricity bills depends on the system's location and load profile. This has been demonstrated in Refs. [30,31] and the results presented in this

paper. As a rule of thumb, when the majority of costly load happens in summer, the tilt should be small. Thus, the PV array can harvest the radiation of the elevated sun in summer. The opposite can be concluded for heating-dominated loads in winter. For azimuth, the daily load profile is considered. The PV array should be faced more to the east when costly load occurs mainly before noon. The same can be concluded when maximum profit is searched wherein the GCPVS owner can benefit from the revenues from the energy sold. The optimum orientation relies on the supportive policy, i.e., the PV array should be oriented to ensure high energy generation over the great FiT rate.

Finally, the novel analysis of this paper is given in Figs. 7 and 9 when optimization is conducted to find the maximum peak load shaving. Under this orientation, although GCPVS generates less energy than the one with the maximum yield, it shaves more of the peak load. This is highlighted in Fig. 7 (e) and (f) for Delft and Fig. 9 (e) and (f) for Mashhad. The results of this analysis can be wisely exploited for policy regulation. Fig. 10 shows an example of modifying fixed FiT into the two-level FiT to motivate system owners to orient their GCPVS into the optimum solution with maximum peak load shaving. These daily data are extracted from Mashhad, analyzed in Section 3, and slightly

Table 4Comparison of this paper with existing literature.

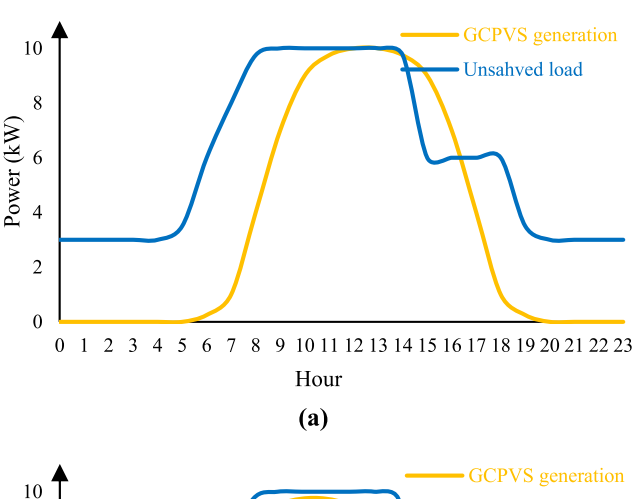
•		
Optimization target	Main conclusion of the literature	Obtained results in this work
Maximum annual yield [25,27]	 β = close to the location's latitude ψ = a function of the longitude angle minus the absolute latitude angle (i. e., ψ ~ 0° for northern hemisphere). 	 32° ≤ β ≤ 35° and ψ = 0° for Mashhad with 36.2972° N, 59.6067° E β = 41° and ψ = 0° for Delft with 52.0116° N, 4.3571° E Fig. 6 (a) and 8 for cases that all orientations are not viable
Minimum electricity bills [30,31]	Optimum solution depends on load profile and GCPVS's site	 Not applicable to Mashhad since no net metering policy exists 30° ≤ β ≤ 50° and −30° ≤ ψ ≤ 30° for Delft
Maximum profit (revenues) [32, 33]	Results mainly depends on the policy and GCPVS's site	 32° ≤ β ≤ 35° and ψ = 0° for Mashhad Not applicable to Delft since no FiT policy exists
Maximum peak load shaving	No studies has been conducted	 32° ≤ β ≤ 35° and ψ = 0° for Mashhad (since electricity rate is fixed over the time, result is the same of max. annual yield) 30° ≤ β ≤ 50° and −30° ≤ ψ ≤ 30° for Delft

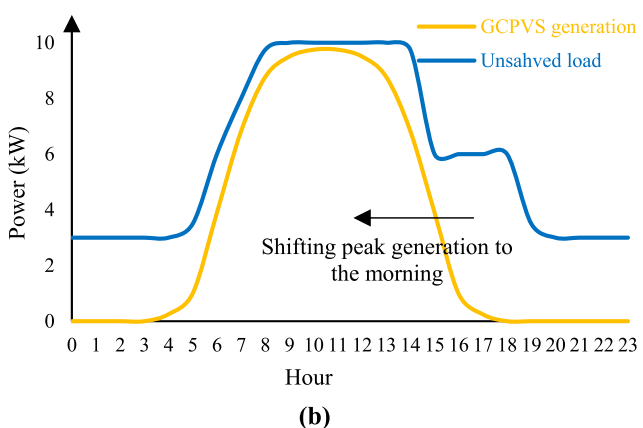
manipulated. Fig. 10 (a) depicts a daily-unshaved load (141.5 kWh) and GCPVS generation. The peak load ($P_L \geq 5$ kW) is 77.5 kWh, which can be shaved by 60.5 kWh when the GCPVS is oriented to have the maximum annual yield (it is the same as maximum profit under fixed FiT). To ensure maximum peak load shaving, the GCPVS generation should coincide with the peak load. When the FiT would be greater for such duration (e.g., 0.030 ϵ /kWh for non-peak and 0.042 ϵ /kWh for peak hours), orienting PV array to the southeast is economically feasible. In this case, the GCPVS shaves 69.7 kWh of the peak load. Note that the two-level FiT is designed so that the paid incentive would be the same for both cases, i.e., 3.2 ϵ for the considered day (Table 5). It is worth noting that the same analysis can be performed over a longer timeframe such as a year.

4.2. Limitations and potential improvements

The proposed optimization method needs meteorological measurement, characteristics of the PV module and inverter (already presented by manufacturers), and load profile. Despite the advantages described above, this work has a few technical and practical limitations:

- The tilt and azimuth might be restricted in some applications, such as rooftop systems in the Netherlands with limited space. Thus, orienting the PV modules to the optimum solution might not be feasible. In the proposed work, the solutions are sorted considering the fitness function, i.e., Fig. 7 (a) and (b) for Delft and Fig. 9 (a) and (b) for Mashhad. Hence, among the feasible solutions (i.e., the ones in which the PV module can be oriented), the designer/installer can choose the tilt and azimuth with the greatest peak load shaving. Thus, the approach is still beneficial, even if the optimum solution cannot be chosen.
- The terms in Section 2.2 are based on non-partial shading scenarios; hence, the method suffers from errors when the studied GCPVS frequently experiences partial shading, e.g., caused by a tree, nearby building, and chimney. As a future work, an improved PV module model can be used so that such applications would also be supported.
- The method needs a load profile of the studied case over a year. In some applications, household and commercial buildings connected





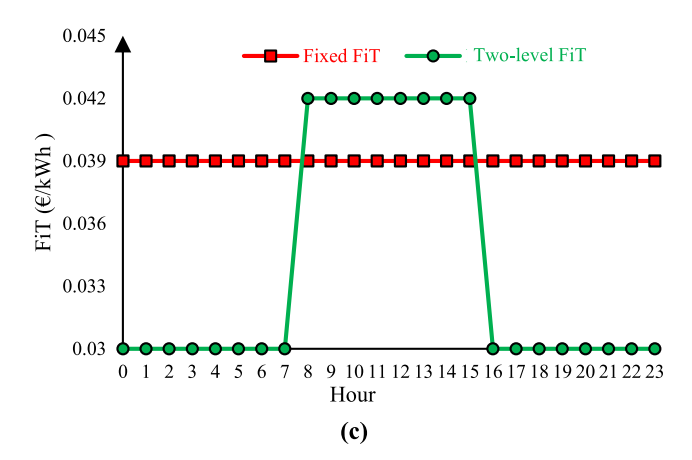


Fig. 10. Results for fixed and dynamic FiT schemes: a) Daily GCPVS generation and load profile with maximum annual yield, b) Daily GCPVS generation and load profile with maximum peak load shaving, c) Daily rates for fixed and dynamic FiT.

to distribution voltage levels, access to such data might be restricted due to the intellectual properties (IP). However, such data are usually supported at regional and national scales, e.g., Refs. [53,54] in France and the Netherlands, both with 15-min resolution.

Future work can enhance this research in multiple directions. First, although the solution time of the proposed algorithm is not long since the search is not exhaustive, the search region can be reduced to further speed up the solution method. In this context, the load profile can be preanalyzed to restrict the β and ψ search limits. For the studied Iranian household case, for example, the maximum peak load occurs at summer noon, implying a small level for tilt angle and near 0° for azimuth (facing

Table 5Summary of the results for the fixed and dynamic FiT scheme.

Policy	GCPVS energy	Load demand	Unshaved load during peak hours $(P_L \ge 8 \text{ kW})$	Peak load shaved by GCPVS	Incentive paid
Fixed FiT (0.039 €/kWh)	82 kWh	141.5 kWh	77.5 kWh	60.5 kWh	3.2 €/day
Two-level FiT (0.030 €/kWh for non-peak and 0.042 €/kWh for peak hours)	80 kWh			69.7 kWh	3.2 €/day

South). Hence, the search area can be chosen as $0^\circ \le \beta \le 30^\circ$ and $-20^\circ \le \psi \le +20^\circ$, significantly reducing the search area. In addition, the method can be re-structured as a two-stage decision process: the first stage with a large step change for β and ψ to find the candidate ranges, and the second stage with a small step change to seek the optimum solution(s) within those ranges. This can also reduce the search region, boosting the efficiency of the method without losing accuracy.

Second, the application range of the proposed method can be extended. Here, the optimization is performed for a predefined GCPVS and load profile. As a direction for future research, the size and electrical design of GCPVS can also be considered as decision variables. Hence, the size and design of GCPVS affect its annual generated energy in Eq. (5). Also, electrical limitations in GCPVS design should be considered as constraints. According to the equations in Section 2.2, the PV module's output power is computed considering the uniform received irradiance, making the method prone to errors under partial shading condition. This can be addressed in future research by modeling the site's shading objects (e.g., trees, a chimney, and nearby buildings) in the energy calculation process so that all pivotal variables affecting the peak load shaving level can be considered within the optimization.

Finally, although the outputs are computed for either maximizing the peak load shaving or maximizing the benefit from the incentive, the combination of these goals can be considered in the objective function in Eq. (5). That is, x_1 , x_2 , x_3 , and x_4 can be non-binary, e.g., $x_3 = 0.5$ and $x_4 = 0.5$ for the studied Dutch building to optimize the peak load and electricity bills simultaneously. Moreover, installing the PV array with the optimum solution may not be feasible due to the site's shading objects since such modeling is excluded in this work. Nonetheless, the best answers can be sorted, similar to Figs. 7 and 9. For example, the solutions with a 5% deviation from the maximum peak load shaving can be defined, and the feasible one in this range can be chosen.

5. Conclusions

Effective peak load shaving can be adopted to address the technical and economic challenges of the electrical power system over-design, ensuring a reliable electricity supply. Deploying residential and power plant GCPVSs is a solid approach; however, this technology should be designed optimally to match its supply (generation) with local demand. This paper tackles this problem by optimizing the tilt and azimuth angles of the fixed GCPVS to achieve the maximum peak load shaving. The methodology searches for the optimum solution within the feasible ranges, considering an accurate GCPVS energy estimation model.

The methodology is implemented in two cities, Delft and Mashhad, with a moderate marine climate (peak load in cold afternoons) and semiarid climate (peak load in summer noon), respectively. The simulation outputs demonstrate that the studied GCPVS does not generate the maximum annual energy by the found optimum solution; however, the level and duration of the peak load are reduced the most under these selections. The outputs provide valuable insights to the power system owners and policymakers to foster such installations. This necessitates collecting the load data (at the selected scale) and conducting the optimization. One example of future incentives would be considering multi-level FiT depending on the time instead of a fixed FiT. The FiT should be greater at durations of the peak load so that the GCPVSs are pushed to have high generated energy in these time intervals. Such high energy generation can be fulfilled by choosing PV tilt and azimuth at the optimum one, determined by the proposed method.

The calculation process can be further sped up by pre-analyzing the studied load (reducing the search region) and re-arranging a two-stage approach (with a larger step in the first stage to quickly find the candidate ranges). More variables, such as PV size, can be engaged in the formulation to extend the application range. The presented methodology requires minimal input data, all available in several databases/vendors' datasheet. This method can also be applied to all GCPVS sizes and load profiles. Due to the wide application range of the proposed work, from residential to regional and national scales, it can be considered as an efficient multi-scale approach for maximizing peak load shaving.

CRediT authorship contribution statement

Reza Bakhshi-Jafarabadi: Writing – review & editing, Writing – original draft, Supervision, Methodology, Formal analysis, Conceptualization. **Christian Doh Dinga:** Writing – original draft, Validation, Methodology.

Declaration of competing interest

The authors declare that they have no known competing financial interests or personal relationships that could have appeared to influence the work reported in this paper.

References

- IRENA. International Renewable Energy Agency, Global energy transformation: a roadmap to 2050. www.irena.org, 2018.
- [2] M. Arslan, M. Çunkaş, An experimental study on determination of optimal tilt and orientation angles in photovoltaic systems, J. Eng. Res. (Kuwait) (2024), https://doi.org/10.1016/j.jcs.2024.07.015
- [3] R. Bakhshi-Jafarabadi, J. Sadeh, A. Soheili, Global optimum economic designing of grid-connected photovoltaic systems with multiple inverters using binary linear programming, Sol. Energy 183 (2019) 842–850, https://doi.org/10.1016/j. solener.2019.03.019.
- [4] Y. Tian, C.Y. Zhao, A review of solar collectors and thermal energy storage in solar thermal applications, Appl. Energy 104 (2013) 538–553, https://doi.org/10.1016/ j.apenergy.2012.11.051.
- [5] J. Kumar, N.R. Parhyar, M.K. Panjwani, D. Khan, Design and performance analysis of PV grid-tied system with energy storage system, Int. J. Electr. Comput. Eng. 11 (2021) 1077–1085, https://doi.org/10.11591/ijece.v11i2.pp1077-1085.
- [6] D. Boruah, S. Singh Chandel, A comprehensive analysis of eight rooftop gridconnected solar photovoltaic power plants with battery energy storage for enhanced energy security and grid resiliency, Sol. Energy 266 (2023), https://doi. org/10.1016/j.solener.2023.112154.
- [7] M. Morey, N. Gupta, M.M. Garg, A. Kumar, A comprehensive review of gridconnected solar photovoltaic system: architecture, control, and ancillary services, Renew. Energy Focus 45 (2023) 307–330, https://doi.org/10.1016/j. ref.2023.04.009.
- [8] R. Ito, S. Lee, Development of adjustable solar photovoltaic system for integration with solar shading louvers on building façades, Appl. Energy 359 (2024), https://doi.org/10.1016/j.apenergy.2024.122711.
- [9] M. Obeng, S. Gyamfi, N.S. Derkyi, A.T. Kabo-bah, F. Peprah, Technical and economic feasibility of a 50 MW grid-connected solar PV at UENR Nsoatre campus, J. Clean. Prod. 247 (2020), https://doi.org/10.1016/j.jclepro.2019.119159.
- [10] G. Sharma, Anjali, A review on grid-connected PV system, Int. J. Trend Sci. Res. Dev. 1 (2017) 2456–6470. www.ijtsrd.com.
- [11] M. Karimi, H. Mokhlis, K. Naidu, S. Uddin, A.H.A. Bakar, Photovoltaic penetration issues and impacts in distribution network - a review, Renew. Sustain. Energy Rev. 53 (2016) 594–605, https://doi.org/10.1016/j.rser.2015.08.042.
- [12] M. Mao, L. Zhang, H. Huang, B. Chong, L. Zhou, Maximum power exploitation for grid-connected PV system under fast-varying solar irradiation levels with modified salp swarm algorithm, J. Clean. Prod. 268 (2020), https://doi.org/10.1016/j. jclepro.2020.122158.

- [13] K.Y. Lau, C.W. Tan, K.Y. Ching, The implementation of grid-connected, residential rooftop photovoltaic systems under different load scenarios in Malaysia, J. Clean. Prod. 316 (2021), https://doi.org/10.1016/j.jclepro.2021.128389.
- [14] M. Hossain, S. Mekhilef, M. Danesh, L. Olatomiwa, S. Shamshirband, Application of extreme learning machine for short term output power forecasting of three gridconnected PV systems, J. Clean. Prod. 167 (2017) 395–405, https://doi.org/ 10.1016/j.iclepro.2017.08.081.
- [15] M. Hartner, A. Ortner, A. Hiesl, R. Haas, East to west the optimal tilt angle and orientation of photovoltaic panels from an electricity system perspective, Appl. Energy 160 (2015) 94–107, https://doi.org/10.1016/j.apenergy.2015.08.097.
- [16] A. Awasthi, A.K. Shukla, S.R. Murali Manohar, C. Dondariya, K.N. Shukla, D. Porwal, G. Richhariya, Review on sun tracking technology in solar PV system, Energy Rep. 6 (2020) 392–405, https://doi.org/10.1016/j.egyr.2020.02.004.
- [17] A. Bahrami, C.O. Okoye, U. Atikol, The effect of latitude on the performance of different solar trackers in Europe and Africa, Appl. Energy 177 (2016) 896–906, https://doi.org/10.1016/j.apenergy.2016.05.103.
- [18] R. Ben Mansour, M.A. Mateen Khan, F.A. Alsulaiman, R. Ben Mansour, Optimizing the solar PV tilt angle to maximize the power output: a case study for Saudi Arabia, IEEE Access 9 (2021) 15914–15928, https://doi.org/10.1109/ ACCESS.2021.3052933.
- [19] S. Soulayman, M. Hammoud, Optimum tilt angle of solar collectors for building applications in mid-latitude zone, Energy Convers. Manag. 124 (2016) 20–28, https://doi.org/10.1016/j.enconman.2016.06.066.
- [20] G. Liu, M.G. Rasul, M.T.O. Amanullah, M.M.K. Khan, Techno-economic simulation and optimization of residential grid-connected PV system for the Queensland climate, Renew. Energy 45 (2012) 146–155, https://doi.org/10.1016/j. renene.2012.02.029.
- [21] J.H. Lucio, R. Valdés, L.R. Rodrí guez, Loss-of-load probability model for standalone photovoltaic systems in Europe, Sol. Energy 86 (2012) 2515–2535, https:// doi.org/10.1016/j.solener.2012.05.021.
- [22] K. Osmani, M. Ramadan, T. Lemenand, B. Castanier, A. Haddad, Optimization of PV array tilt angle for minimum levelized cost of energy, Comput. Electr. Eng. 96 (2021), https://doi.org/10.1016/j.compeleceng.2021.107474.
- [23] M. Agrawal, P. Chhajed, A. Chowdhury, Performance analysis of photovoltaic module with reflector: optimizing orientation with different tilt scenarios, Renew. Energy 186 (2022) 10–25, https://doi.org/10.1016/j.renene.2021.12.149.
- [24] A.Z. Hafez, A. Soliman, K.A. El-Metwally, I.M. Ismail, Tilt and azimuth angles in solar energy applications – a review, Renew. Sustain. Energy Rev. 77 (2017) 147–168, https://doi.org/10.1016/j.rser.2017.03.131.
- [25] F. Jafarkazemi, S.A. Saadabadi, Optimum tilt angle and orientation of solar surfaces in Abu Dhabi, UAE, Renew. Energy 56 (2013) 44–49, https://doi.org/ 10.1016/i.renene.2012.10.036.
- [26] Y. Lv, P. Si, X. Rong, J. Yan, Y. Feng, X. Zhu, Determination of optimum tilt angle and orientation for solar collectors based on effective solar heat collection, Appl. Energy 219 (2018) 11–19, https://doi.org/10.1016/j.apenergy.2018.03.014.
- [27] W.G. Le Roux, Optimum tilt and azimuth angles for fixed solar collectors in South Africa using measured data, Renew. Energy 96 (2016) 603–612, https://doi.org/ 10.1016/j.renene.2016.05.003
- [28] N. Lu, J. Qin, Optimization of tilt angle for PV in China with long-term hourly surface solar radiation, Renew. Energy 229 (2024), https://doi.org/10.1016/j. renene.2024.120741.
- [29] V. Shekar, D. Abraham, A. Caló, E. Pongrácz, Determining the optimal azimuth for solar-ready buildings: simulating for maximising the economic value of solar PV installations in Lapland, Finland, Renew. Energy 241 (2025), https://doi.org/ 10.1016/j.renep. 2025 122357
- [30] J.D. Rhodes, C.R. Upshaw, W.J. Cole, C.L. Holcomb, M.E. Webber, A multiobjective assessment of the effect of solar PV array orientation and tilt on energy production and system economics, Sol. Energy 108 (2014) 28–40, https://doi.org/ 10.1016/j.solener.2014.06.032.
- [31] I.H. Rowlands, B.P. Kemery, I. Beausoleil-Morrison, Optimal solar-PV tilt angle and azimuth: an Ontario (Canada) case-study, Energy Policy 39 (2011) 1397–1409, https://doi.org/10.1016/j.enpol.2010.12.012.
- [32] M. Hummon, P. Denholm, R. Margolis, Impact of photovoltaic orientation on its relative economic value in wholesale energy markets, Prog. Photovoltaics Res. Appl. 21 (2013) 1531–1540, https://doi.org/10.1002/pip.2198.

- [33] J.E. Haysom, K. Hinzer, D. Wright, Impact of electricity tariffs on optimal orientation of photovoltaic modules, Prog. Photovoltaics Res. Appl. 24 (2016) 253–260, https://doi.org/10.1002/pip.2651.
- [34] M. Bortolini, M. Gamberi, A. Graziani, Technical and economic design of photovoltaic and battery energy storage system, Energy Convers. Manag. 86 (2014) 81–92, https://doi.org/10.1016/j.enconman.2014.04.089.
- [35] B. Ceran, J. Jurasz, A. Mielcarek, P.E. Campana, PV systems integrated with commercial buildings for local and national peak load shaving in Poland, J. Clean. Prod. 322 (2021), https://doi.org/10.1016/j.jclepro.2021.129076.
- [36] Y. Li, W. Gao, Y. Ruan, Performance investigation of grid-connected residential PV-battery system focusing on enhancing self-consumption and peak shaving in Kyushu, Japan, Renew. Energy 127 (2018) 514–523, https://doi.org/10.1016/j.renepe 2018.04.074
- [37] J. Alpízar-Castillo, V. Vega-Garita, N. Narayan, L. Ramirez-Elizondo, Open-access model of a PV-BESS system: quantifying power and energy exchange for peakshaving and self consumption applications, Energies 16 (2023), https://doi.org/ 10.3390/en16145480.
- [38] A. Ashoornezhad, H. Falaghi, A. Hajizadeh, M. Ramezani, Feasibility study on the integration of residential PV-battery systems in system peak load shaving: a case study in Iran, IET Gener. Transm. Distrib. 17 (2023) 3100–3113, https://doi.org/ 10.1049/gtd2.12878.
- [39] W.L. Schram, I. Lampropoulos, W.G.J.H.M. van Sark, Photovoltaic systems coupled with batteries that are optimally sized for household self-consumption: assessment of peak shaving potential, Appl. Energy 223 (2018) 69–81, https://doi.org/ 10.1016/j.apenergy.2018.04.023.
- [40] S.M.S. Mousavi, R. Bakhshi-Jafarabadi, Techno-economic assessment of grid-connected photovoltaic systems for peak shaving in arid areas based on experimental data, Energy Rep. 11 (2024) 5492–5503, https://doi.org/10.1016/j.eour.2024.05.035
- [41] NREL-national solar radiation database. https://nsrdb.nrel.gov/data-viewer, 2024. (Accessed 24 May 2024).
- [42] PVGIS, (n.d.). https://re.jrc.ec.europa.eu/pvg_tools/en/(accessed May 24, 2024).
- [43] Solar API and weather forecasting tool, (n.d.). https://www.solcast.com/?gad_sou rce=1&gclid=EAIaIQobChMIu829wZHThgMVI6doCR2a8gxQEAAYASAAEg LXI_D_BwE (accessed November 18, 2024).
- [44] B. Nayak, A. Mohapatra, K.B. Mohanty, Parameter estimation of single diode PV module based on GWO algorithm, Renew. Energy Focus 30 (2019) 1–12, https://doi.org/10.1016/j.ref.2019.04.003.
- [45] S. Bogning Dongue, D. Njomo, L. Ebengai, A new strategy for accurately predicting I-V electrical characteristics of PV modules using a nonlinear five-point model, J. Energy 2013 (2013) 1–8, https://doi.org/10.1155/2013/321694.
- [46] G.A. Rampinelli, A. Krenzinger, F. Chenlo Romero, Mathematical models for efficiency of inverters used in grid connected photovoltaic systems, Renew. Sustain. Energy Rev. 34 (2014) 578–587, https://doi.org/10.1016/j. rser.2014.03.047.
- [47] R. Bakhshi-Jafarabadi, J. Sadeh, M. Dehghan, Economic evaluation of commercial grid-connected photovoltaic systems in the Middle East based on experimental data: a case study in Iran, Sustain. Energy Technol. Assessments 37 (2020), https://doi.org/10.1016/j.seta.2019.100581.
- [48] MEEDC. https://www.meedc.ir/, 2024. (Accessed 18 November 2024).
- [49] MFFBAS. https://www.mffbas.nl/documenten/, 2024. (Accessed 18 November 2024).
- [50] Historical weather data. www.timeanddate.com/weather, 2025, 2025.
- [51] JAM72S30 525-550. https://www.jasolar.com/uploadfile/2021/0706/2021070 6053524693.pdf, 2025.
- [52] Sunny tripower 10.0-3. https://www.sma.de/en/products/solarinverters/sunn y-tripower-80-100, 2024. (Accessed 10 October 2024).
- [53] https://www.services-rte.com/en/view-data-published-by-rte.html, 2025 accessed on March 2025.
- [54] https://netztransparenz.tennet.eu/electricity-market/transparency-pages/tran sparency-germany/network-figures/annual-peak-load-and-load-curve/, 2025 accessed on March 2025.